

Appearance of bulk Superconductivity under Hydrostatic Pressure in
 $\text{Sr}_{0.5}\text{RE}_{0.5}\text{FBiS}_2$ (RE = Ce, Nd, Pr and Sm) new compounds

Rajveer Jha, Brajesh Tiwari and V.P.S. Awana*

CSIR-National Physical Laboratory, Dr. K.S. Krishnan Marg, New Delhi-110012, India

Abstract

We report the appearance of superconductivity under hydrostatic pressure (0.35–2.5GPa) in $\text{Sr}_{0.5}\text{RE}_{0.5}\text{FBiS}_2$ with RE = Ce, Nd, Pr and Sm. The studied compounds, synthesized by solid state reaction route, are crystallized in tetragonal $P4/nmm$ space group. At ambient pressure though the RE = Ce exhibit the onset of superconductivity below 2.5K, the Nd, Pr and Sm samples are not superconducting down to 2K. With application of hydrostatic pressure (up to 2.5GPa), superconducting transition temperature (T_c) is increased to around 10K for all the studied samples. The magneto-transport measurements are carried out on all the samples with maximum T_c i.e., at under 2.5GPa pressure and their upper critical fields (H_{c2}) are determined. The new superconducting compounds appear to be quite robust against magnetic field but within Pauli paramagnetic limit. The new superconducting compounds with various RE (Ce, Nd, Pr and Sm) belonging to $\text{Sr}_{0.5}\text{La}_{0.5}\text{FBiS}_2$ family are successfully synthesized for the first time and superconductivity is induced in them under hydrostatic pressure.

Keywords: BiS₂ based new superconductors, structure, Effects of pressure, Transport properties and Transition temperature variation.

PACS number(s): 74.10.+v, 74.70.-b, 74.62.Fj, 74.70. Dd, 74.62.-c

***Corresponding Author**

Dr. V. P. S. Awana, Principal Scientist

E-mail: awana@mail.nplindia.org

Ph. +91-11-45609357, Fax-+91-11-45609310

Homepage www.fteewebs.com/vpsawana/

Introduction

BiS₂ based superconductivity was first observed at around 4.5K in BiS₂ layers of Bi₄O₄S₃ compound [1,2]. Later the same was seen in REO/FBiS₂ [3-12] compounds. In short span of time, the BiS₂ based superconductivity attracted tremendous interest from the scientific community [1-12]. The principal reason for the same is the layered structure of these compounds being similar to that of famous REO/FFeAs pnictides high T_c superconductors. In case of REO/FBiS₂ the charge carriers (p-type) are introduced by O²⁻ site F¹⁻ substitution in REO redox layer and superconductivity is established in adjacent BiS₂ layer. This is exactly same as being done in case of REO/FFeAs, where O/F substitution in REO redox layers introduces superconductivity in adjacent FeAs layer [13]. It is also reported that the BiS₂ based superconductivity of REO/FBiS₂ systems does enhance tremendously under hydrostatic pressure [14-17]. The increase in superconducting transition temperature (T_c) has been reported even up to five fold or so. For example the T_c of LaO_{0.5}F_{0.5}BiS₂ increases from around 2.1K to above 10K under hydrostatic pressure of say above 2GPa [14,18]. Researchers also synthesized the high pressure high temperature (HPHT) processed compounds of REO/FBiS₂ series and established stable superconductivity of up to 10K [16]. As far as theoretical aspects are concerned, detailed electronic structure calculations are made and the role of sp orbitals of Bi and S are highlighted [19-21]. The situation seems to be in parallel with Fe and As hybridization in case of Fe Pnictide (REO/FFeAs) superconductors [13]. No doubt, the BiS₂ based recent superconductivity is catching the attention of scientific community [1-12, 14-22].

It is proposed earlier that the ground state of the REO/FBiS₂ system is a similar structure compound SrFBiS₂ [23]. In SrFBiS₂, the carriers (e-type) are introduced by Sr²⁺ site La³⁺ substitution, and superconductivity is achieved of up to 2.5K [24-26]. Interestingly, though in case of REO/FBiS₂ superconductivity is reported for RE=La, Pr, Nd and Ce [3-12], in SrFBiS₂ series only Sr_{1-x}La_xBiS₂ is yet studied [24-26]. It was thus required to check upon the SrFBiS₂ series with Sr site different RE substitutions. Further though the p-type REO/FBiS₂ superconductivity is studied for various RE [3-12, 14-18], the same need to be probed for e-type Sr/RE substituted SrFBiS₂, with various RE other than the reported RE=La [24-25]. The only other report on evolution of superconductivity via e-type carriers is by substitution of tetravalent Th⁺⁴, Hf⁺⁴, Zr⁺⁴, and Ti⁺⁴ for trivalent La⁺³ in LaOBiS₂ compound [27]. Recently we found that

superconducting transition temperature (T_c) of $\text{Sr}_{0.5}\text{La}_{0.5}\text{BiS}_2$ increased five-fold from around 2K to above 10K accompanied with a semiconducting to metallic transformation in normal state under just above 1GPa external pressure [28]. Keeping all this in mind, in current article we report successful synthesis of $\text{Sr}_{0.5}\text{RE}_{0.5}\text{FBiS}_2$ with RE = Ce, Nd, Pr and Sm compounds for first time and study their superconducting properties with and without application of hydrostatic pressure. It is found that though RE=Pr and Sm do not show superconductivity down to 2K, the RE=Ce exhibited the onset of superconductivity below say 2.5K. Interestingly, all the RE exhibited superconductivity of up to 10K under hydrostatic pressure. Their magneto-transport measurements showed that these are quite robust against magnetic field. This is the first study on synthesis and appearance of bulk superconductivity in $\text{RE}_{0.5}\text{Sr}_{0.5}\text{FBiS}_2$ systems with RE other La.

Experimental details

The bulk polycrystalline samples of series $\text{Sr}_{0.5}\text{RE}_{0.5}\text{FBiS}_2$ (RE = Ce, Nd, Pr and Sm) were synthesized by solid state reaction route via vacuum encapsulation. High purity Ce, Nd, Pr, Sm, SrF_2 , Bi and S were weighed in stoichiometric ratio and ground in pure Argon atmosphere glove box. The mixed powders were subsequently palletized and vacuum-sealed (10^{-4} mbar) in different quartz tubes. The box furnace was used to sinter the samples at 650°C for 12h with the typical heating rate of $2^\circ\text{C}/\text{min}$. The sintered samples were subsequently cooled down slowly to room temperature. This process was repeated twice. X-ray diffraction (XRD) patterns were recorded for all samples at room temperature in the scattering angular (2θ) range of 10° - 80° in equal 2θ step of 0.02° using *Rigaku Diffractometer* with $\text{Cu } K_\alpha$ ($\lambda = 1.54\text{\AA}$). Rietveld analysis was performed for all samples using the standard *FullProf* program.

The pressure dependent resistivity measurements were performed on Physical Property Measurements System (*PPMS-14T, Quantum Design*) using HPC-33 Piston type pressure cell with Quantum design DC resistivity Option. Hydrostatic pressures were generated by a BeCu/NiCrAl clamped piston-cylinder cell. The sample was immersed in a pressure transmitting medium (Daphne Oil) covered with a Teflon cell. Annealed Pt wires were affixed to gold-sputtered contact surfaces on each sample with silver epoxy in a standard four-wire configuration.

Results

The room temperature observed and Reitveld fitted XRD pattern for the $\text{Sr}_{0.5}\text{RE}_{0.5}\text{FBiS}_2$ (RE=Ce, Nd, Pr and Sm) compounds are shown in figure 1. All the compounds are crystallized in tetragonal structure with space group $P4/nmm$. Small impurity peak of Bi_2S_3 are also observed in $\text{Sr}_{0.5}\text{Sm}_{0.5}\text{FBiS}_2$ compound, which are close to the background of XRD pattern. On the other hand all the other studied samples are mostly phase pure within the XRD limit. Reitveld fitted lattice parameters are $a=4.068(1)$ Å, $c=13.36(2)$ Å for $\text{Sr}_{0.5}\text{Ce}_{0.5}\text{FBiS}_2$; $a=4.056(3)$ Å, $c=13.38(2)$ Å for $\text{Sr}_{0.5}\text{Nd}_{0.5}\text{FBiS}_2$; $a=4.61(2)$ Å, $c=13.36(1)$ Å for $\text{Sr}_{0.5}\text{Pr}_{0.5}\text{FBiS}_2$ and $a=4.054(1)$ Å, $c=13.40(3)$ Å for $\text{Sr}_{0.5}\text{Sm}_{0.5}\text{FBiS}_2$ compounds. The volume of the unit cell obtained through the Reitveld fitting analysis of each compound and other parameters, including their atomic co-ordinate positions are summarized in the table 1. The volume of unit cell is increasing with the increasing ionic radii of the RE element from Sm to Ce. There is a possibility of internal chemical pressure on the unit cell of $\text{Sr}_{0.5}\text{RE}_{0.5}\text{FBiS}_2$, similar to that as in the case of $\text{REO}_{0.5}\text{F}_{0.5}\text{BiS}_2$ [3, 5, 10] with different RE.

The temperature dependent electrical resistivity $\rho(T)$ for the $\text{Sr}_{0.5}\text{RE}_{0.5}\text{FBiS}_2$ (RE=Ce, Nd, Pr and Sm) compounds in the temperature range 2-300K is shown in figure 2. All the compounds show the semiconducting behavior down to 2K, except the $\text{Sr}_{0.5}\text{Ce}_{0.5}\text{FBiS}_2$ compound, which exhibits the superconducting transition (T_c^{onset}) near the 2.7K, while the $\rho=0$ not attained down to 2K, please see figure 2. It is expected that the superconducting transition temperature (T_c) may increase with replacing La to Nd, Ce, Pr and Sm, as in the case of $\text{REO}_{0.5}\text{F}_{0.5}\text{BiS}_2$ [3, 10]. Interestingly, the T_c^{onset} is absent down to 2K in these compounds, except for RE = Ce, which exhibited T_c^{onset} near 2.7K. Seemingly, the chemical pressure on the unit cell is not large enough to bring in superconductivity in these compounds. This is the reason that we applied external pressure on the studied $\text{Sr}_{0.5}\text{RE}_{0.5}\text{FBiS}_2$ compounds and achieved superconductivity in them .for first time

Figure 3a shows temperature dependent electrical resistivity $\rho(T)$ at various applied pressure of 0.35-2.5GPa in the temperature range 2-300K for the $\text{Sr}_{0.5}\text{Ce}_{0.5}\text{FBiS}_2$ compound. The normal state resistivity shows the semiconducting behavior at the applied pressure of

0.35GPa, which is suppressed remarkably with increasing pressure of up to 1.5GPa. The normal state resistivity completely changes from semiconducting to the metallic one at 2.0GPa and 2.5GPa applied pressures. Inset of the figure 3a shows the superconducting transition at various pressures. At 0.35GPa, the T_c^{onset} appears at 2.8K, it looks like the same as the ambient pressure data but with reduced resistivity and the $T_c(\rho=0)$ is not seen down to 2K. The $T_c(\rho=0)$ above 2K can be seen at the pressure 0.55GPa with the T_c^{onset} at 4K. The $T_c(\rho=0)$ increases from 2K to 3K at 0.97GPa with T_c^{onset} at 6K, having sufficient broadening in the superconducting transition. At the 1.5GPa the superconductivity increases to T_c^{onset} at 9.7K with $T_c(\rho=0)$ at 8.5K, for the 2.0GPa pressure the T_c^{onset} is 9.9K with $T_c(\rho=0)$ at around 9K, and the same are nearly unchanged for 2.5GPa pressure.

Figure 3b shows $\rho(T)$ for the $\text{Sr}_{0.5}\text{Nd}_{0.5}\text{FBiS}_2$ compound in the temperature range 2-300K at various applied pressures of 0.35-2.5GPa. The semiconducting behavior of normal state resistivity also observed in the $\text{Sr}_{0.5}\text{Nd}_{0.5}\text{FBiS}_2$ compound, for the studied pressures from 0.35GPa to 1.5GPa but with decreasing resistivity. The semiconducting to metallic transition has been observed at the 2.0GPa, and is followed for the further higher pressure of 2.5GPa as well. Inset is the zoomed part of figure 3b in the temperature range 14-2K. At pressure 0.35GPa the T_c^{onset} appears at 2.5K, which is absent at the ambient pressure data down to 2K. The $T_c(\rho=0)$ above 2K is seen at 0.55GPa with the T_c^{onset} at 3.5K. At 0.97GPa the $T_c(\rho=0)$ slightly increases from 2K to 2.5K and the T_c^{onset} is seen at around 5.8K, with broadened superconducting transition width. For the 1.5GPa pressure $T_c(\rho=0)$ is 4.5K and the T_c^{onset} is at 9.25K, with sufficient broadening of the superconducting transition. This broadening in the superconducting transition disappears at the 2.0GPa pressure with $T_c(\rho=0)$ at 8.7K, and T_c^{onset} is 9.5K. For the further applied pressure 2.5GPa T_c is slightly increased with same onset, thus resulting in a sharper superconducting transition.

The temperature dependent electrical resistivity at various applied pressure for the $\text{Sr}_{0.5}\text{Pr}_{0.5}\text{FBiS}_2$ is shown in the figure 3c. In $\text{Sr}_{0.5}\text{Pr}_{0.5}\text{FBiS}_2$ as well the semiconducting to metallic transition has been observed at 2.0GPa. Inset is the zoomed part of figure 3c in the temperature range 14-2K. Interestingly, at 0.35GPa the compound shows $T_c(\rho=0)$ near 2K, and T_c^{onset} is above 2.7K. At 0.55GPa pressure T_c^{onset} slightly increases to 2.9K. In case of 0.97GPa, the $T_c(\rho=0)$ is above 2.5K and the T_c^{onset} is at 6K, resulting in a broadened superconducting

transition width. At 1.5GPa the superconductivity is enhanced with T_c^{onset} at 9.7K and $T_c(\rho=0)$ at 8.5K. For the 2.0GPa pressure the T_c^{onset} is 10K with $T_c(\rho=0)$ at 9K, and the superconducting transition is sharp. For 2.5GPa pressure, the T_c^{onset} is unaltered but the $T_c(\rho=0)$ is slightly decreased.

The $\rho(T)$ from 300K to 2K at various applied pressure for the $\text{Sr}_{0.5}\text{Sm}_{0.5}\text{FBiS}_2$ is shown in the figure 3d. The $\text{Sr}_{0.5}\text{Sm}_{0.5}\text{FBiS}_2$ compound shows the similar nature as for above studied three different RE, i.e., semiconducting to metallic transition at or above the 2.0GPa. So, it can be said that the 2.0GPa is transition (semiconducting to metallic) pressure for $\text{Sr}_{0.5}\text{RE}_{0.5}\text{FBiS}_2$ compounds. Inset of figure 3d is zoomed part of figure 3a in the superconducting region 14-2K. The $\text{Sr}_{0.5}\text{Sm}_{0.5}\text{FBiS}_2$ compound shows the T_c^{onset} at 2.4K at 0.35GPa and 2.8K at pressure 0.55GPa, but no $T_c(\rho=0)$. At 0.97GPa pressure, the T_c^{onset} is near 5.6K, and $T_c(\rho=0)$ is above 2.2K. At the 1.5GPa pressure T_c^{onset} slightly increases up to 9.1K and the $T_c(\rho=0)$ above 3.5K, having large transition width at the this pressure. For the further higher pressure of 2.0GPa the T_c^{onset} is at 9.4K and $T_c(\rho=0)$ at 8.0K. At 2.5GPa the superconducting transition is more sharper with slight decrease in the T_c^{onset} to 9.2K and $T_c(\rho=0)$ increasing to at 8.3K.

Figure 4 shows the Pressure dependence of the superconducting transition temperature T_c^{onset} for the $\text{Sr}_{0.5}\text{RE}_{0.5}\text{FBiS}_2$ (RE=Ce, Nd, Pr and Sm) compounds. It can be inferred that superconductivity gradually increases with pressure up to the 0.97GPa, for all the samples. For higher pressure of 1.5GPa, the T_c^{onset} shoots up to above 9K. It seems that 1.5GPa is the transition pressure (P_t) for all the samples. With further increase in the pressure, though the T_c^{onset} gets almost saturated, the $T_c(\rho=0)$ is increased, resulting in relatively sharper superconducting transition widths in pressure range of 1.5-2.5GPa. In our results we also observed slight decreases in T_c^{onset} for $\text{Sr}_{0.5}\text{Ce}_{0.5}\text{FBiS}_2$ and $\text{Sr}_{0.5}\text{Sm}_{0.5}\text{FBiS}_2$ samples at the 2.5GPa pressure, otherwise the trend of enhancement of superconductivity under pressure is same for all the samples.

Figure 5(a-d) shows the $\rho(T)$ under applied magnetic fields (1-7Tesla) for the $\text{Sr}_{0.5}\text{RE}_{0.5}\text{FBiS}_2$ (RE=Ce, Nd, Pr and Sm) compounds at applied pressure of 2.5GPa. Here, it can be seen that the T_c^{onset} decreases less compared to $T_c(\rho=0)$ with the increasing magnetic field. In these compounds the superconducting transition width is broadened under applied magnetic

fields. The upper critical field H_{c2} has been estimated from the resistivity drop 90% the normal state resistance $\rho_n(T,H)$ at T_c^{onset} in applied magnetic fields for all the samples. The upper critical field at absolute zero temperature $H_{c2}(0)$ is determined by using the conventional one-band Werthamer–Helfand–Hohenberg (*WHH*) equation, i.e., $H_{c2}(0) = -0.693T_c(dH_{c2}/dT)_{T=T_c}$. The estimated $H_{c2}(0)$ are 13.8Tesla, 11.6Tesla, 13.5Tesla and 14.5Tesla for $\text{Sr}_{0.5}\text{Ce}_{0.5}\text{FBiS}_2$, $\text{Sr}_{0.5}\text{Nd}_{0.5}\text{FBiS}_2$, $\text{Sr}_{0.5}\text{Pr}_{0.5}\text{FBiS}_2$ and $\text{Sr}_{0.5}\text{Sm}_{0.5}\text{FBiS}_2$ respectively. As shown in figure 6, the solid lines are the extrapolation to the Ginzburg–Landau equation $H_{c2}(T)=H_{c2}(0)(1-t^2/1+t^2)$, where $t=T/T_c$ is the reduced temperature, which gives values slightly higher than that by WHH approach. These upper critical field values for all samples are close to but within the Pauli paramagnetic limit i.e. $H_p=1.84T_c$.

Discussion

Early rare-earth substituted BiS_2 -based layered compounds $\text{Sr}_{0.5}\text{RE}_{0.5}\text{FBiS}_2$ (RE=Ce, Nd, Pr and Sm) are crystallized in tetragonal structure with space group $P4/nmm$. The choice of different RE-ions in these $\text{Sr}_{0.5}\text{RE}_{0.5}\text{FBiS}_2$ (RE=Ce, Nd, Pr and Sm) compounds is based on the fact that the superconductivity has been reported in $\text{Sr}_{0.5}\text{La}_{0.5}\text{FBiS}_2$ increased from 2.5K to 10K under external hydrostatic pressure [28]. It is important to note that there is no effect of different RE-ions on the c lattice parameter however a lattice parameter decreases as the ionic radii of RE-ion in $\text{Sr}_{0.5}\text{RE}_{0.5}\text{FBiS}_2$ decreases monotonically. Under ambient pressure they all show the semiconducting normal state with minimum resistivity for $\text{Sr}_{0.5}\text{Pr}_{0.5}\text{FBiS}_2$ at room temperature. Apart from $\text{Sr}_{0.5}\text{Ce}_{0.5}\text{FBiS}_2$ none of the studied compounds showed onset of superconducting transition in the measured temperature ranges 300K to 2K. Under hydrostatic pressure starting from 0.35GPa to 2.50GPa all these compounds showed superconductivity of whom superconducting onset temperature (T_c^{onset}) seems to saturate above 1.5GPa at 9K to 10K for $\text{Sr}_{0.5}\text{RE}_{0.5}\text{FBiS}_2$ (RE=Ce, Nd, Pr and Sm). The sharp increase in T_c^{onset} up to 1.5 GPa pressure and its saturation above further application of pressure suggests some type of structural changes in these Pauli paramagnetic limited ($H_p\sim 1.84T_c$) superconductors. Based on structural and magnetic studies, Tomita et.al [29] have argued in a BiS_2 -based compound $\text{LaO}_{1-x}\text{F}_x\text{BiS}_2$, that a sudden increase of T_c with pressure is related to the structural transition from tetragonal to monoclinic. The significant increases in the T_c as well as the suppression of semiconducting behavior in the normal state resistivity suggest increase in the charge carrier density in the

pressure range 0.35-1.5GPa. For $\text{LnO}_{0.5}\text{F}_{0.5}\text{BiS}_2$ (Ln-La, Ce) compounds, C. T. Wolowiec et. al have suggested the possibility of coexistence of two phases near the pressure $\sim 1.0\text{GPa}$ causing the broadening in the superconducting transition and further increase of pressure suppresses the low transition phase [16]. The similar behavior also observed in these compounds in the pressure range 0.35-1.5GPa. To rule out the possibility of strong correlation of electrons in these compounds, which go semiconducting to metal transition with pressure along a sharp increase in T_c needs to be confirmed with detailed structural analysis. In a study on single crystal of $\text{PrO}_{0.5}\text{F}_{0.5}\text{BiS}_2$ the normal state resistivity changes from semiconducting-like behavior to metallic behavior under pressure and T_c increases from 3.5K to 8.5K [30]. In a recently appeared preprint Morice et.al, has predicted for a similar set of compounds $\text{LnO}_{1-x}\text{F}_x\text{BiS}_2$ (Ln = La, Ce, Pr, and Nd) especially CeOBiS_2 that they should display a pressure induced semiconducting to metal transition also the change of rare-earth does not affect the Fermi surface from the first principles studies [31]. The resistivity under magnetic field at the pressure of 2.5GPa exhibited a decrease in T_c with increasing magnetic field, clearly suggesting that these compounds are type-II superconductor. The upper critical fields determined by WHH models are close to but within the Pauli paramagnetic limit i.e. $H_p=1.84T_c$.

In summary, we have synthesized layered fluorosulfide compounds $\text{Sr}_{0.5}\text{RE}_{0.5}\text{FBiS}_2$ (RE = Ce, Nd, Pr and Sm) for first time, which crystallized in tetragonal $P4/nmm$ space group. These compounds are semiconductors in the temperature range 300-2K at ambient pressure and become metallic under pressure at P_t (1.5GPa). All the compounds show superconductivity under hydrostatic pressure of up to the maximum T_c^{onset} above 10K for the $\text{Sr}_{0.5}\text{Pr}_{0.5}\text{FBiS}_2$ compound. In resistivity under magnetic field measurements at the applied pressure 2.5GPa these compounds appear to be robust against magnetic field but yet within the Pauli paramagnetic limit.

Authors would like to thank their Director NPL India for his keen interest in the present work. This work is financially supported by *DAE-SRC* outstanding investigator award scheme on search for new superconductors. Rajveer Jha acknowledges the *CSIR* for the senior research fellowship.

Reference:

1. Y. Mizuguchi, H. Fujihisa, Y. Gotoh, K. Suzuki, H. Usui, K. Kuroki, S. Demura, Y. Takano, H. Izawa, O. Miura, Phys. Rev. B **86**, 220510(R) (2012).
2. S. K. Singh, A. Kumar, B. Gahtori, Shruti; G. Sharma, S. Patnaik, V. P. S. Awana, J. Am. Chem. Soc., **134**, 16504 (2012).
3. Y. Mizuguchi, S. Demura, K. Deguchi, Y. Takano, H. Fujihisa, Y. Gotoh, H. Izawa, O. Miura, J. Phys. Soc. Jpn. **81**, 114725 (2012).
4. J. Xing, S. Li, X. Ding, H. Yang, and H. H. Wen, Phys. Rev. B **86**, 214518 (2012).
5. V.P.S. Awana, A. Kumar, R. Jha, S. K. Singh, A. Pal, Shruti, J. Saha, S. Patnaik, Solid State Communications **157**, 21 (2013).
6. D. Yazici, K. Huang, B.D. White, A.H. Chang, A.J. Friedman and M.B. Maple Philosophical Magazine **93**, 673 (2013).
7. K. Deguchi, Y. Mizuguchi, S. Demura, H. Hara, T. Watanabe, S. J. Denholme, M. Fujioka, H. Okazaki, T. Ozaki, H. Takeya, T. Yamaguchi, O. Miura and Y. Takano, Euro Phys. Lett. **101**, 17004 (2013).
8. R. Jha, A. Kumar, S. K. Singh, V. P. S. Awana, J Supercond Nov Magn. **26**, 499 (2013).
9. R. Jha, H. Kishan, and V.P.S. Awana J. Appl. Phys. **115**, 013902 (2014)
10. S. Demura, Y. Mizuguchi, K. Deguchi, H. Okazaki, H. Hara, T. Watanabe, S. J. Denholme, M. Fujioka, T. Ozaki, H. Fujihisa, Y. Gotoh, O. Miura, T. Yamaguchi, H. Takeya, and Y. Takano, J. Phys. Soc. Jpn. **82**, 033708 (2013).
11. R. Jha and V.P.S. Awana Mat. Res. Exp. 1, 016002 (2014)
12. R. Jha, A. Kumar, S. K. Singh, V.P.S. Awana J. Appl. Phys. **113**, 056102 (2013).
13. Y. Kamihara, T. Watanabe, M. Hirano, H. Hosono, J. Am. Chem. Soc. **130**, 3296 (2008).
14. H. Kotegawa, Y. Tomita, H. Tou, H. Izawa, Y. Mizuguchi, O. Miura, S. Demura K. Deguchi And Y. Takano, Journal of the Physical Society of Japan **81**, 103702 (2012).
15. G. Kalai Selvan, M. Kanagaraj, S. Esakki Muthu, R. Jha, V. P. S. Awana, and S. Arumugam, Phys. Status Solidi RRL **7**, 510 (2013).
16. C. T. Wolowiec, D. Yazici, B. D. White, K. Huang, and M. B. Maple, Phys. Rev. B **88**, 064503 (2013).

17. C. T. Wolowiec, B. D. White, I. Jeon, D. Yazici, K. Huang and M. B. Maple, *J. Phys. Cond. Matt.* **25**, 422201 (2013).
18. H. Sakai, D. Kotajima, K. Saito, H. Wadati, Y. Wakisaka, M. Mizumaki, K. Nitta, Y. Tokura, and S. Ishiwata, *J. Phys. Soc. Jpn.* **83**, 014709 (2014).
19. H. Usui, K. Suzuki, and K. Kuroki *Phys. Rev. B* **86**, 220501(R) (2012).
20. G. Martins, A. Moreo, and E. Dagotto *Phys. Rev. B* **87**, 081102(R) (2013)
21. X. Wan, H.C. Ding, S.Y. Savrasov, and C.G. Duan *Phys. Rev. B* **87**, 115124 (2013).
22. T. Yildirim, *Phys. Rev. B* **87**, 020506(R) (2013).
23. H. Lei, K. Wang, M. Abeykoon, E. S. Bozin, and C. Petrovic, *Inorg. Chem.*, **52**, 10685 (2013).
24. X. Lin, X. Ni, B. Chen, X. Xu, X. Yang, J. Dai, Y. Li, X. Yang, Y. Luo, Q. Tao, G. Cao, Z. Xu, *Phys. Rev. B* **87**, 020504(R) (2013).
25. Y. Li, X. Lin, L. Li, N. Zhou, X. Xu, C. Cao, J. Dai, L. Zhang, Y. Luo, W. Jiao, Q. Tao, G. Cao, Z. Xu, *Sup. Sci. and Tech.* **27**, 935009 (2014).
26. H. Sakai, D. Kotajima, K. Saito, H. Wadati, Y. Wakisaka, M. Mizumaki, K. Nitta, Y. Tokura, and S. Ishiwata, *J. Phys. Soc. Jpn.* **83**, 014709 (2014).
27. D. Yazici, K. Huang, B. D. White, I. Jeon, V. W. Burnett, A. J. Friedman, I. K. Lum, M. Nallaiyan, S. Spagna, M. B. Maple *Phys. Rev. B* **87**, 174512 (2013).
28. R. Jha, Brajesh Tiwari and V.P.S. Awana. *J. Phys. Soc. Jpn.* **83**, 063707 (2014).
29. T. Tomita, M. Ebata, H. Soeda, H. Takahashi, H. Fujihisa, Y. Gotoh, Y. Mizuguchi, H. Izawa, O. Miura, S. Demura, K. Deguchi, Y. Takano, *J. Phys. Soc. Jpn.* **83**, 063704 (2014)
30. M. Fujioka, M. Nagao, S. J. Denholme, M. Tanaka, H. Takeya, T. Yamaguchi, and Y. Takano, arXiv:1406.3888v1.
31. C. Morice, E. Artacho, S. E. Dutton, D. Molnar, H. J. Kim and S. S. Saxena, arXiv:1312.2615v1.

Table 1

Atomic coordinates volume of unit cell, and Wyckoff positions, for studied $\text{Sr}_{0.5}\text{RE}_{0.5}\text{FBiS}_2$ compounds

Samples \rightarrow	$\text{Sr}_{0.5}\text{Ce}_{0.5}\text{FBiS}_2$	$\text{Sr}_{0.5}\text{Nd}_{0.5}\text{FBiS}_2$	$\text{Sr}_{0.5}\text{Pr}_{0.5}\text{FBiS}_2$	$\text{Sr}_{0.5}\text{Sm}_{0.5}\text{FBiS}_2$
χ^2	4.78	4.02	4.81	6.71
$a=b$ (Å)	4.068(1)	4.056(3)	4.061(2)	4.054(1)
c (Å)	13.36(2)	13.38(2)	13.36(1)	13.40(3)
c/a	3.28	3.29	3.28	3.30
$V(\text{Å}^3)$	221.11(2)	220.22(3)	220.52(1)	220.35(3)
Sr/RE(1/4, 1/4, z)	0.110(1)	0.109(2)	0.114(1)	0.113(1)
Bi(1/4, 1/4, z)	0.623(3)	0.624(2)	0.624(3)	0.626(1)
S1(1/4, 1/4, z)	0.379(1)	0.381(1)	0.364(2)	0.363(3)
S2(1/4, 1/4, z)	0.809(2)	0.812(3)	0.810(1)	0.822(1)
F(x,y,z)	(3/4,1/4,0)	(3/4,1/4,0)	(3/4,1/4,0)	(3/4,1/4,0)

Figure Captions

Figure 1: (Color online) Observed (*open circles*) and calculated (*solid lines*) XRD patterns of $\text{Sr}_{0.5}\text{RE}_{0.5}\text{FBiS}_2$ (RE = Ce, Nd, Pr and Sm) compound at room temperature.

Figure 2: (Color online) Resistivity versus temperature $\rho(T)$ plots for $\text{Sr}_{0.5}\text{RE}_{0.5}\text{FBiS}_2$ compounds, at ambient pressure in the temperature range 300K-2.0K. Inset shows the $\rho(T)$ curve in the temperature range 6-2K.

Figure 3(a): (Color online) Resistivity versus temperature $\rho(T)$ plots for $\text{Sr}_{0.5}\text{Ce}_{0.5}\text{FBiS}_2$ compound at various applied pressures (0.35-2.5GPa) in the temperature range 300K-2.0K, inset of each shows the zoomed part of $\rho(T)$ plots near the superconducting transition temperature.

Figure 3(b): (Color online) Resistivity versus temperature $\rho(T)$ plots for $\text{Sr}_{0.5}\text{Nd}_{0.5}\text{FBiS}_2$ compound, at various applied pressures (0.35-2.5GPa) in the temperature range 300K-2.0K, inset of each shows the zoomed part of $\rho(T)$ plots near the superconducting transition temperature.

Figure 3(c): (Color online) Resistivity versus temperature $\rho(T)$ plots for $\text{Sr}_{0.5}\text{Pr}_{0.5}\text{FBiS}_2$ compound at various applied pressures (0.35-2.5GPa) in the temperature range 300K-2.0K, inset of each shows the zoomed part of $\rho(T)$ plots near the superconducting transition temperature.

Figure 3(d): (Color online) Resistivity versus temperature $\rho(T)$ plots for $\text{Sr}_{0.5}\text{Sm}_{0.5}\text{FBiS}_2$ compound at various applied pressures (0.35-2.5GPa) in the temperature range 300K-2.0K, inset of each shows the zoomed part of $\rho(T)$ plots near the superconducting transition temperature.

Figure 4: T_c^{onset} vs applied Pressure for the $\text{Sr}_{0.5}\text{RE}_{0.5}\text{FBiS}_2$ compounds.

Figure 5: (a-d) (Color online) Temperature dependence of the Resistivity $\rho(T)$ under magnetic fields for the $\text{Sr}_{0.5}\text{RE}_{0.5}\text{FBiS}_2$ compound under 2.5GPa hydrostatic pressure.

Figure 6: (Color online) The upper critical field H_{c2} taken from 90%, Resistivity criterion $\rho(T)$ for the $\text{Sr}_{0.5}\text{RE}_{0.5}\text{FBiS}_2$ under 2.5GPa hydrostatic pressure.

Fig. 1

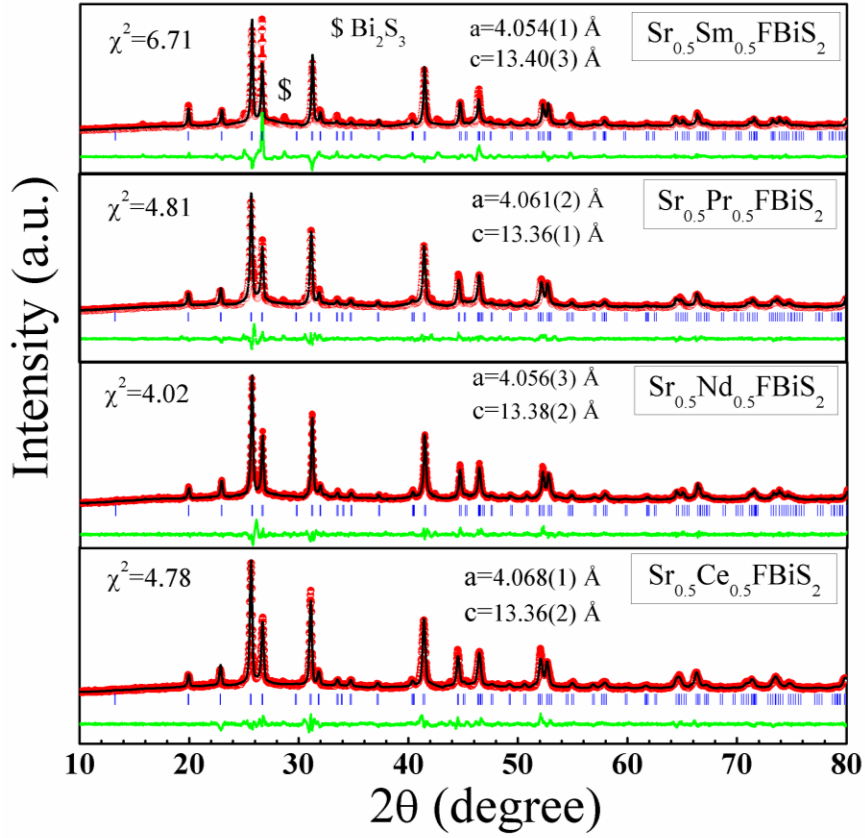


Fig. 2

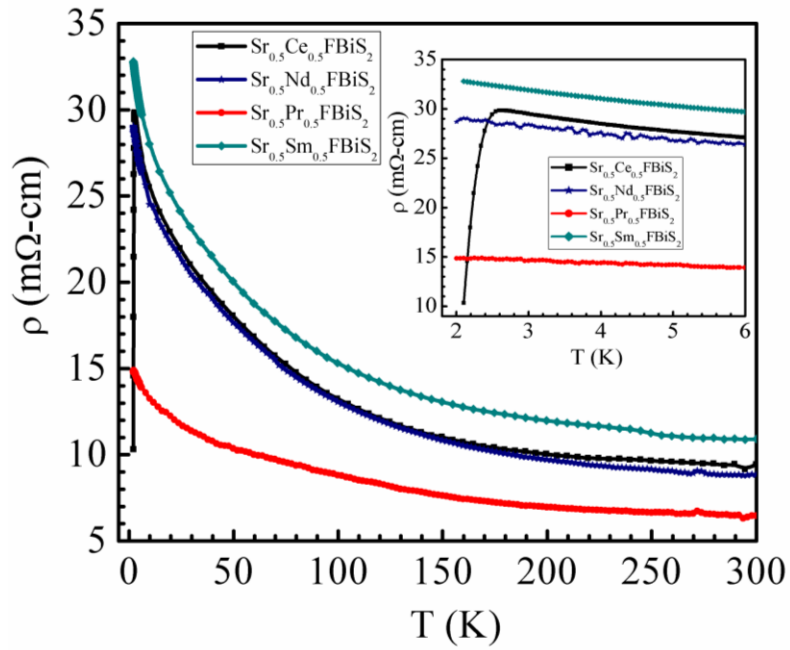


Fig.3 (a)

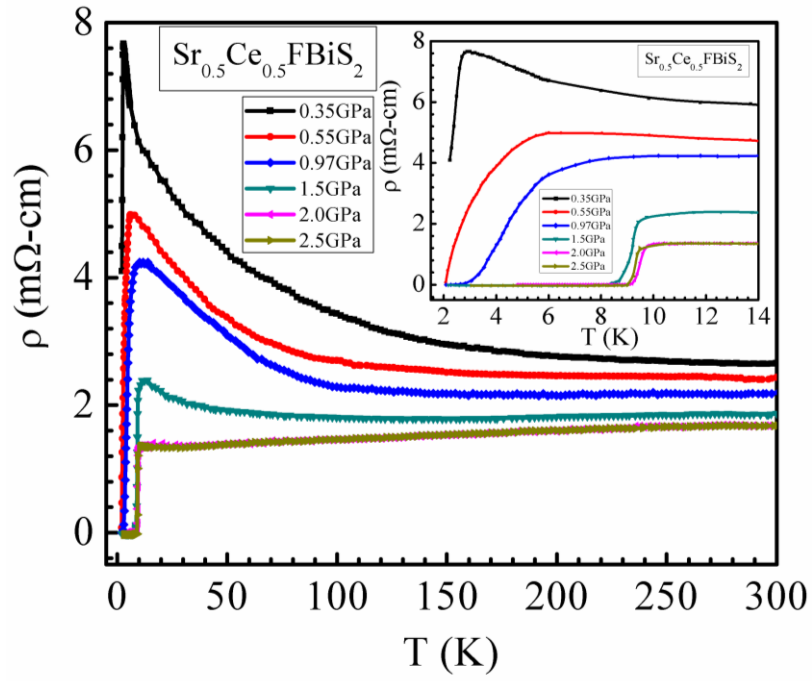


Fig. 3(b)

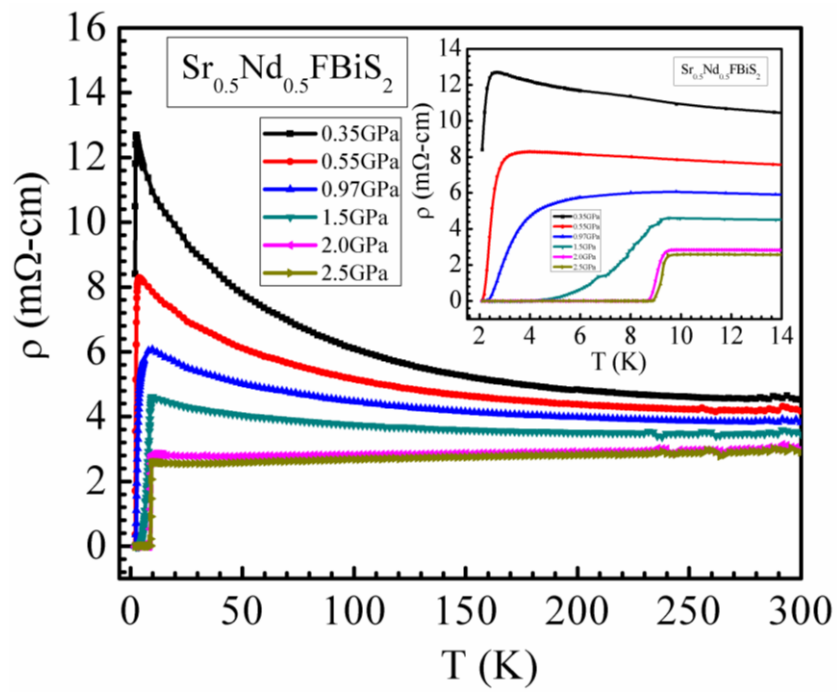


Fig. 3(c)

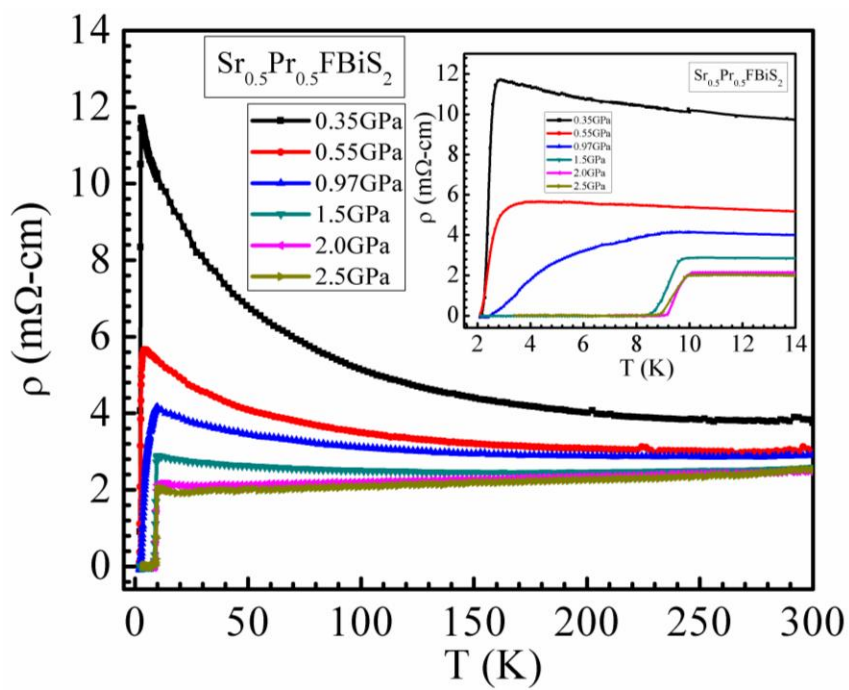


Fig. 3(d)

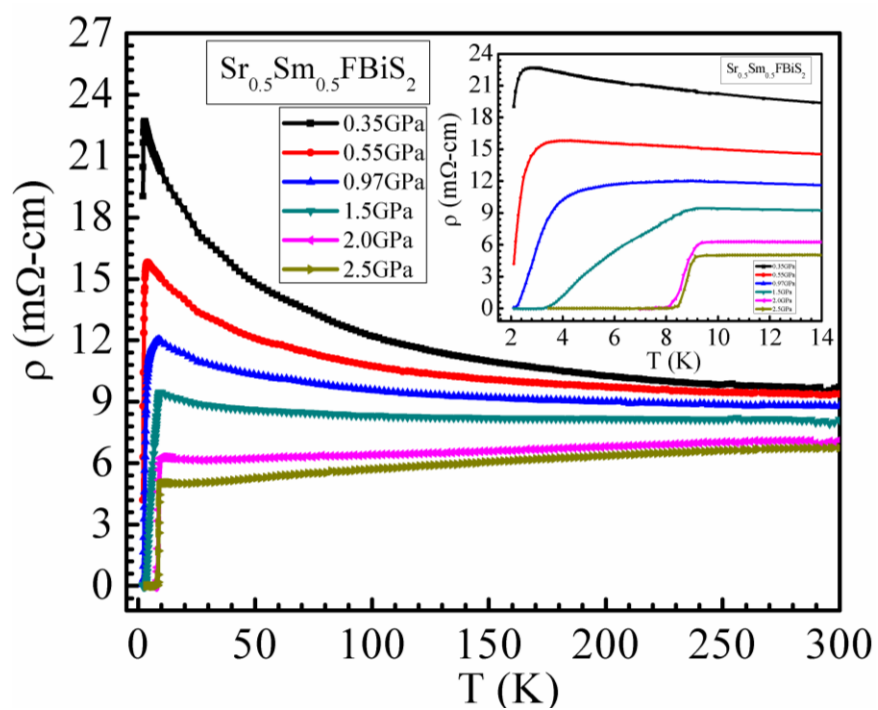


Fig. 4

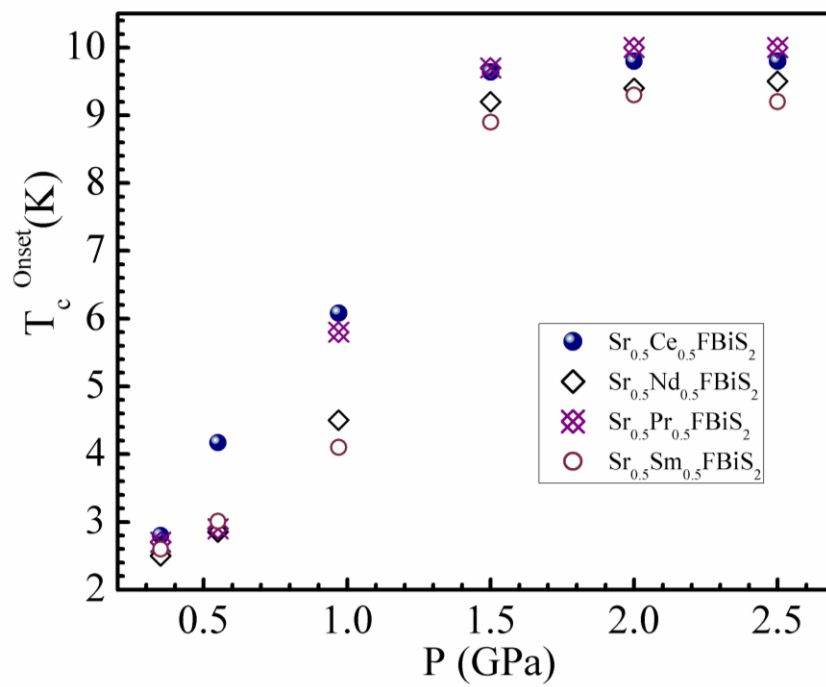
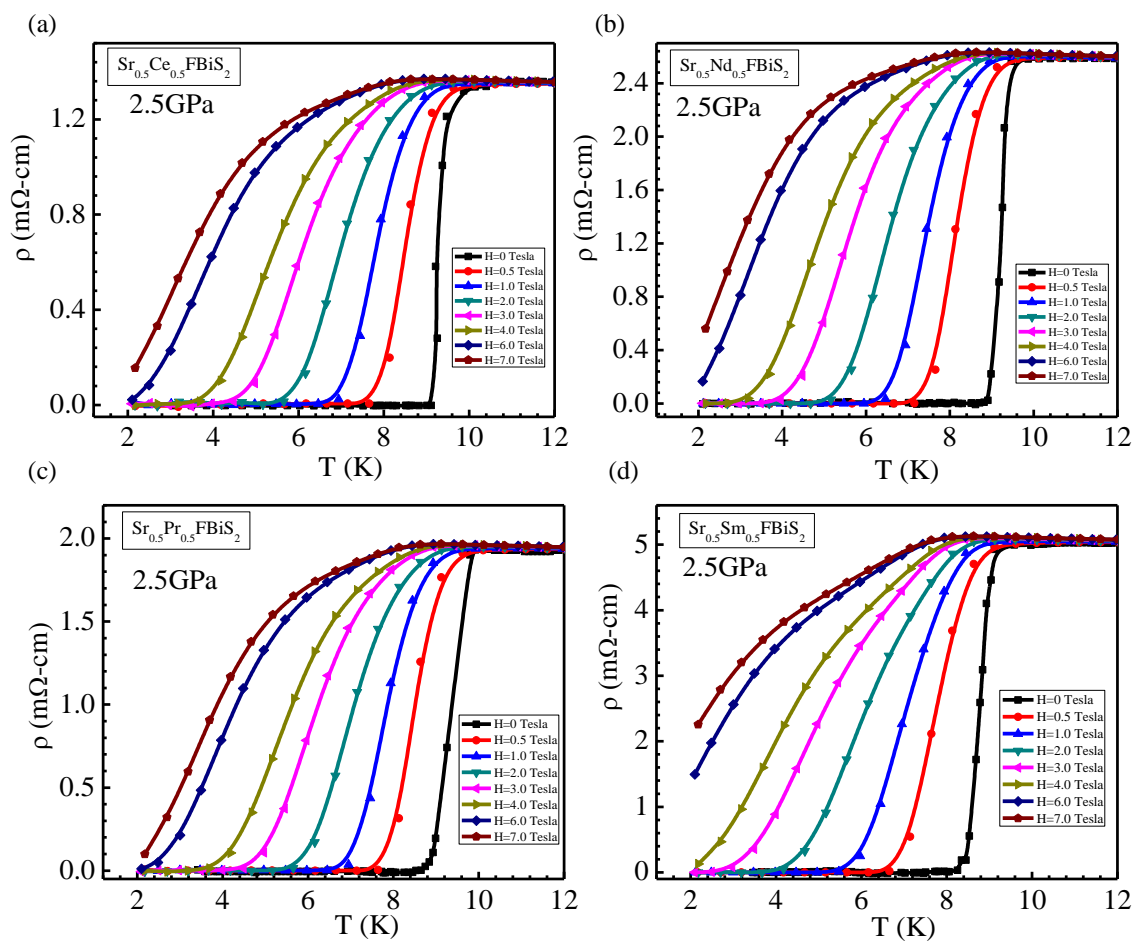


Fig.5**Fig. 6**